Electronic Supplementary Material (ESI) for Physical Chemistry Chemical Physics
This journal is © The Owner Societies 2011

Supporting Information

Correlation of the EPR properties of perchlorotriphenylmethyl radicals and their efficiency as DNP polarizers

Debamalya Banerjee[a], Juan Carlos Paniagua[b], Veronica Mugnaini[c], Jaume Veciana[c], Akiva Feintuch[a], Miquel Pons[d,e], Daniella Goldfarb[a]

[a]Department of Chemical Physics, Weizmann Institute of Science, Rehovot 76100, Israel;
[b]Departament de Química Física & Institut de Química Teòrica i Computacional (IQTC-UB), Universitat de Barcelona. Martí i Franquès 1-11, 08028 Barcelona, Spain.
[c]Institut de Ciència de Materials de Barcelona (ICMAB-CSIC), Bellaterra, Spain and Networking Research Center on Bioengineering, Biomaterials, and NanoMedicine (CIBER-BBN), Bellaterra, Spain.
[d]Departament de Química Orgànica. Universitat de Barcelona. Martí i Franquès 1-11, 08028 Barcelona, Spain.
[e] Institute for Research in Biomedicine (IRB Barcelona), Baldiri Reixac 10-12, 08028 Barcelona, Spain

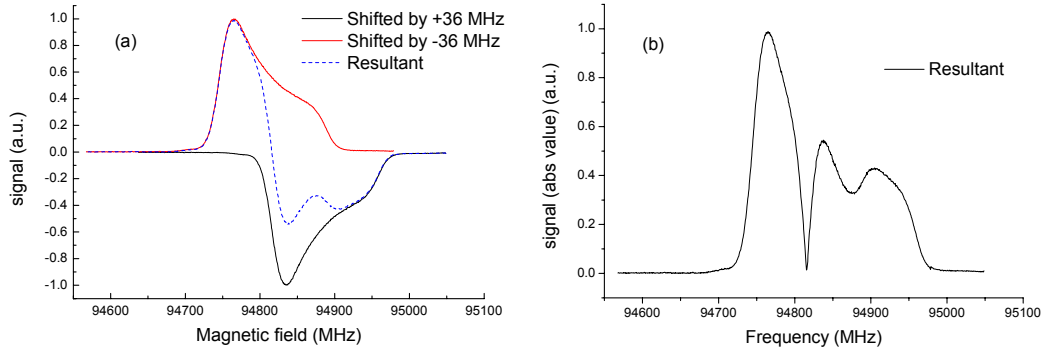

Figure S1: (a) Construction of the ^{13}C DNP frequency sweep from the EPR powder pattern. The ED-EPR spectrum of radical **1** - with the x-axis converted to frequency- has been shifted to both sides by the ^{13}C Larmor frequency (36 MHz at 3.3T Field). The positive-shifted spectrum has been inverted to account for the negative sign of the solid effect. The resultant (dashed blue line) is obtained by numerical addition of these two lines. (b) The absolute value of the calculated ^{13}C DNP frequency sweep (dashed line in a) from the EPR spectrum.

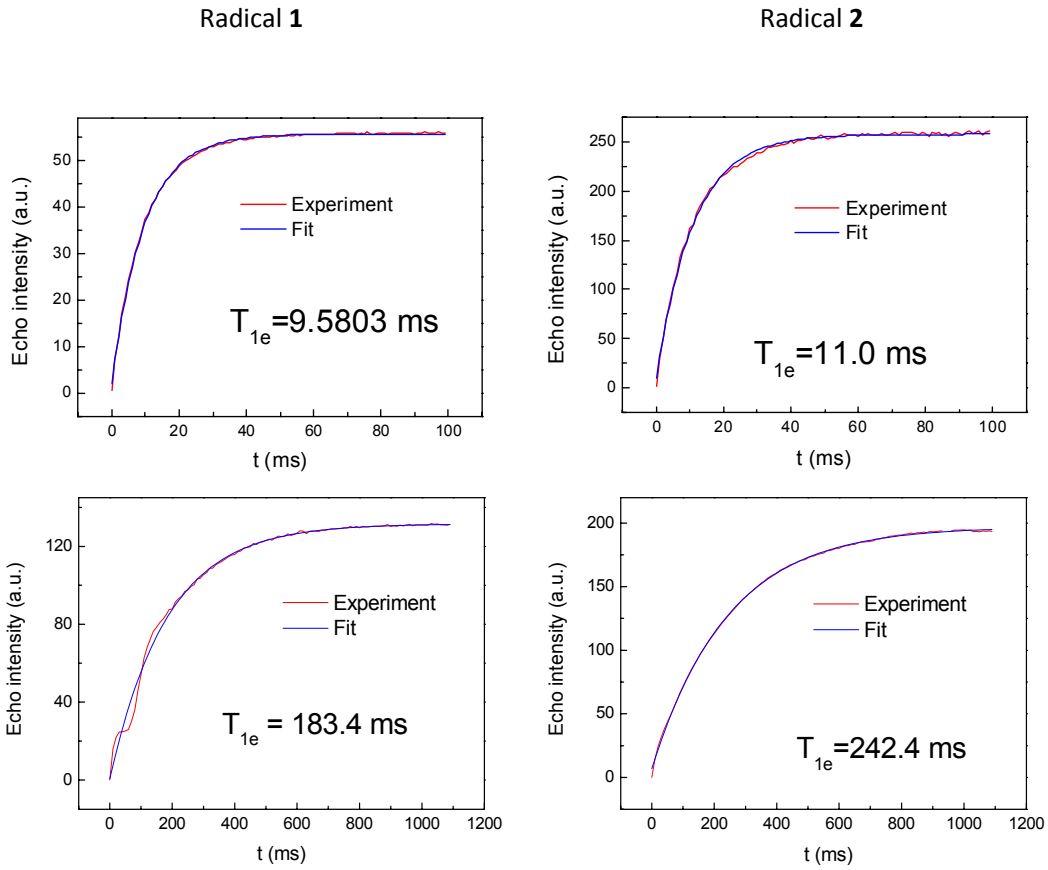

Figure S2: Saturation recovery curves, along with the corresponding single exponential fits, at 40 K (top) and 10 K (bottom) for PTM radicals **1** and **2**. A saturation pulse length of 10 ms has been used.

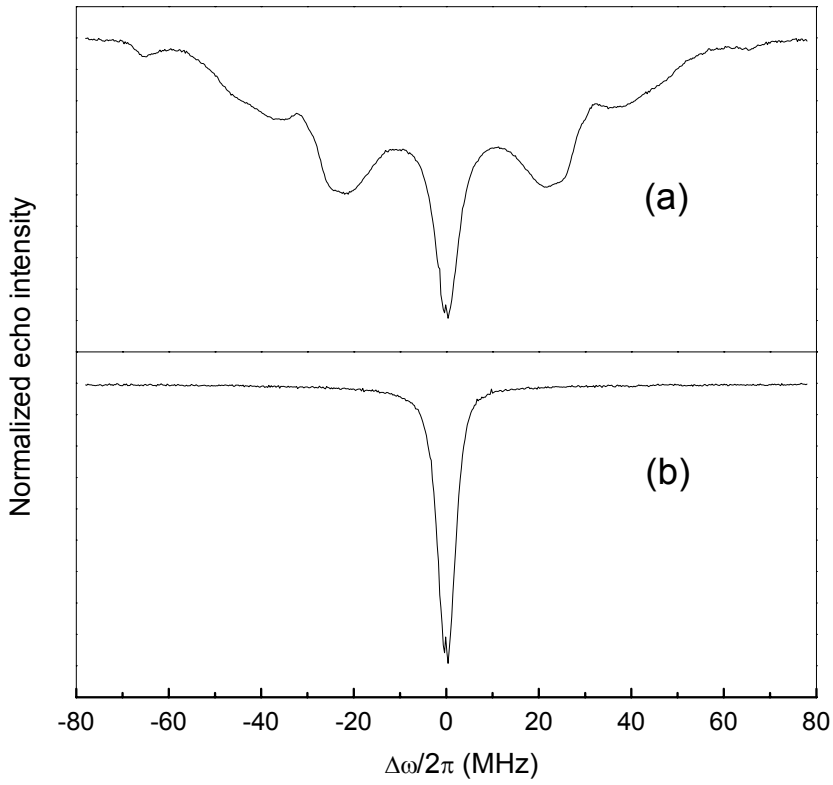

Figure S3: ELDOR-detected NMR spectrum of six *meta* carboxylic acid(-COOH) analogue of radical **2** (a) and of commercially available OX63 (b). Both the spectra were recorded on 1 mM frozen solutions and at $g_{\perp}$. The central line corresponds to the allowed EPR transition (also called the self ELDOR peak). The spectrum corresponding to the proton substituent has very similar features as in the spectrum of radical **2**. No forbidden EPR transitions are seen in the spectrum of OX63.

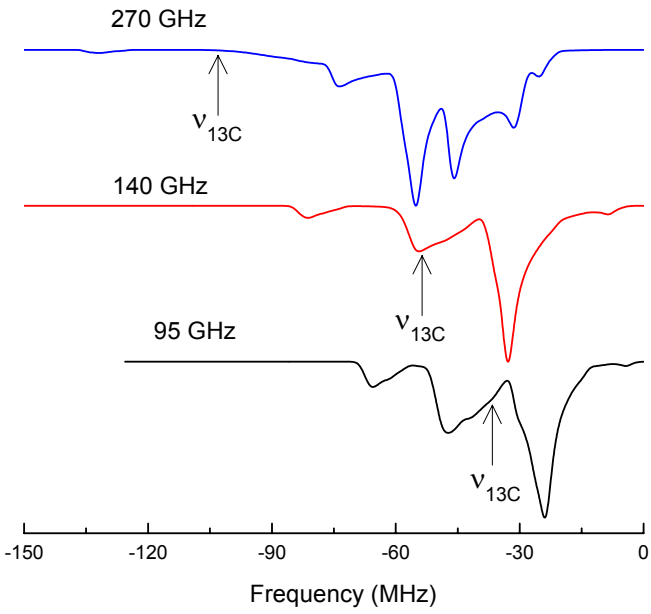

Figure S4: Spectrometer frequency dependence of ENDOR frequencies of ^{35}Cl in Radical 2. Simulations are performed at the $g_{\perp}$ position of the ED-EPR line. Zero frequency corresponds to the allowed EPR transition. The magnetic field is expressed in the corresponding EPR frequencies. For each of the spectrometers frequencies, ν_{13C} is marked with an arrow. At 270 GHz there is hardly any overlap between the ν_{13C} and the ENDOR frequency.

(a)

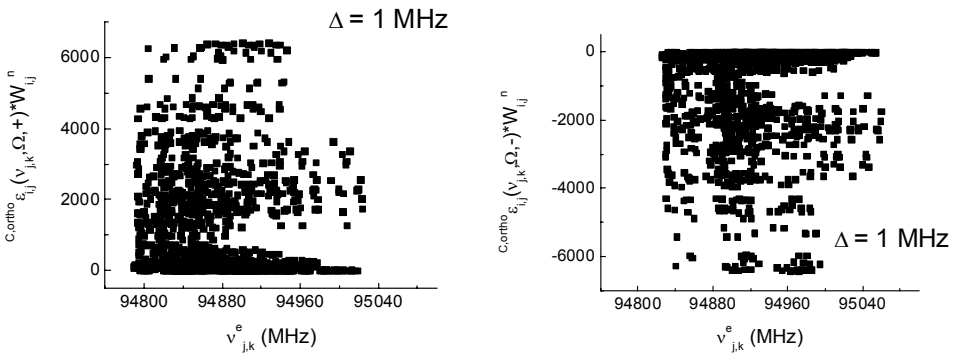

(b)

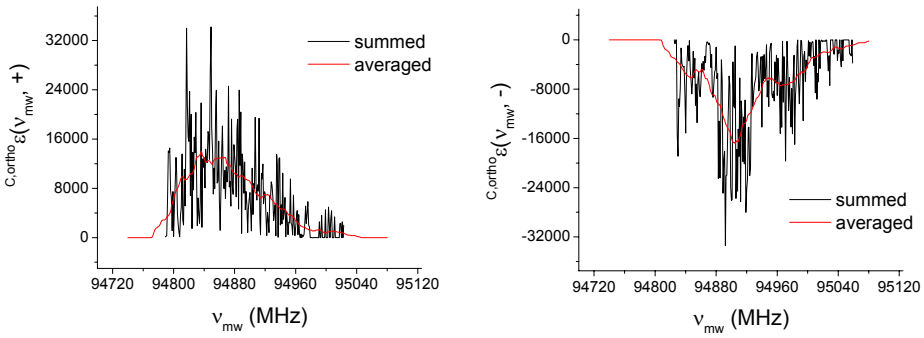

(c)

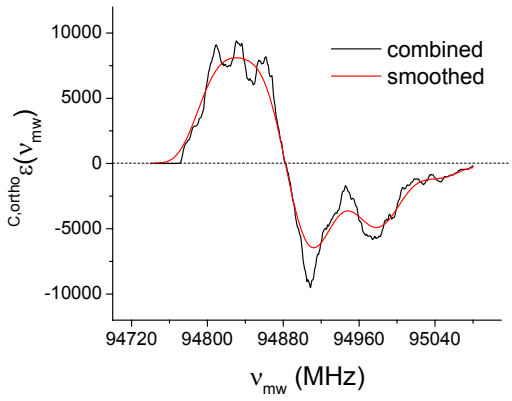

Figure S5: (a) Saturation limit (S→∞) nuclear polarization enhancements $^{Cl,ortho}\varepsilon^{i,j}(\nu_{j,k}, \pm)$, for NMR transitions in the range $\nu_{13C} \pm \Delta$, of the *ortho* ^{35}Cl substituent of radical **2**. The enhancements have been separated into positive (left) and negative (right) and were scaled by the corresponding NMR transition probabilities $W_{i,j}^n$. The data is plotted against the frequency of the corresponding EPR forbidden transitions $\nu_{j,k}^e$. The result was obtained by considering all the

molecular orientations and with a nuclear transition bandwidths value Δ =2.5 MHz. (b) The black line in both panels is obtained from the spectra shown in (a) after binning with δ=0.5 MHz (see Eq. 5a) . The red line is obtained after performing the moving average over the interpolated dataset as mentioned in the text. (c) Combination of the red lines shown in Fig. S5b following equation 6 gives the black curve. The red curve is obtained after smoothing. This line is also shown in Fig. 8(c).

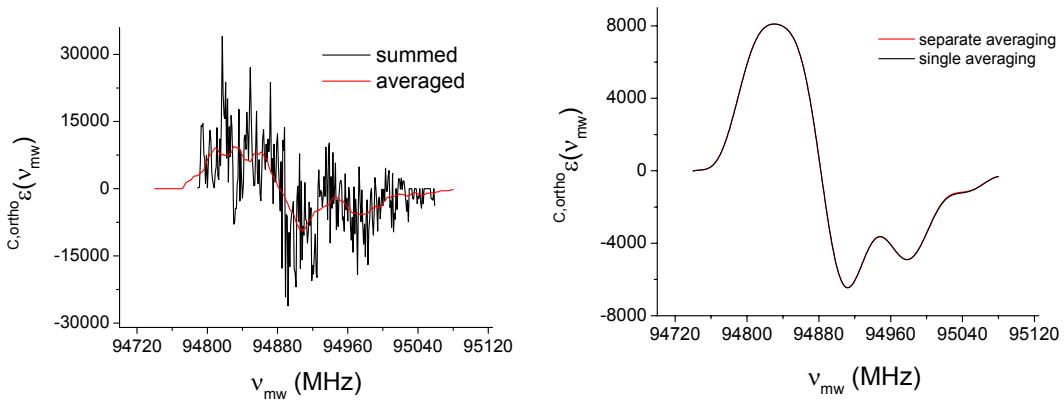

Figure S6: DNP frequency sweep can be obtained without separate treatment of the positive and the negative polarization enhancement values. In the left panel, the data set of figure S5a has been binned without separating into positive and negative values to give the black line. The red line is obtained after moving average over the interpolated data set. Right panel shows the data set after smoothing (black line) and is compared to the smoothed curve obtained by separate treatment of enhancements of different sigh (red line, also shown in S5c). There are hardly any differences between the two traces.

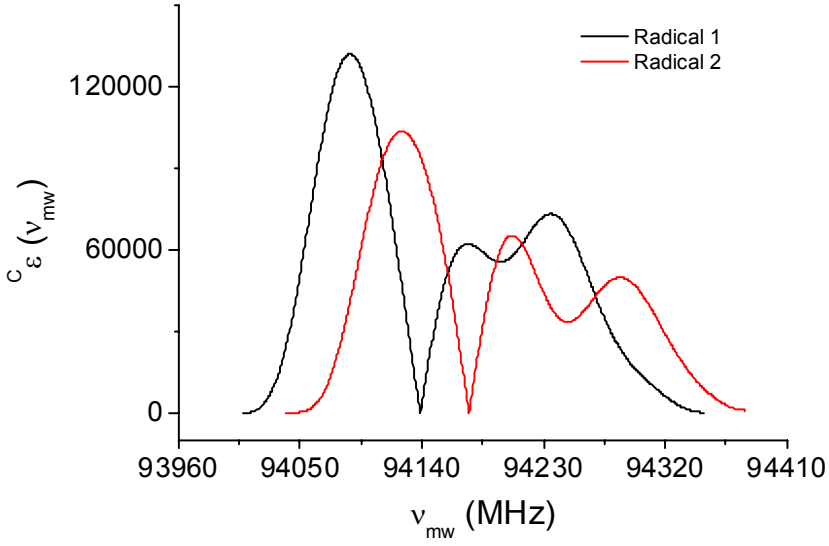

Figure S7: Absolute values of the calculated ^{13}C DNP enhancements radicals **1** and **2**. The calculation has been performed in the saturation limit for one equivalent unit of the PTM radicals, *i.e*. considering 6 *ortho* and 6 *meta* Cl for radical **1** and 6 *ortho* and 3 *para* Cl for radical **2**. Contributions from both Cl isotopes have been added weighted by their natural abundance (~76% for ^{35}Cl and ~24% for ^{37}Cl). Note that the absolute value of the maximum DNP enhancement in radical **1** is higher than the same obtained for radical **2.**

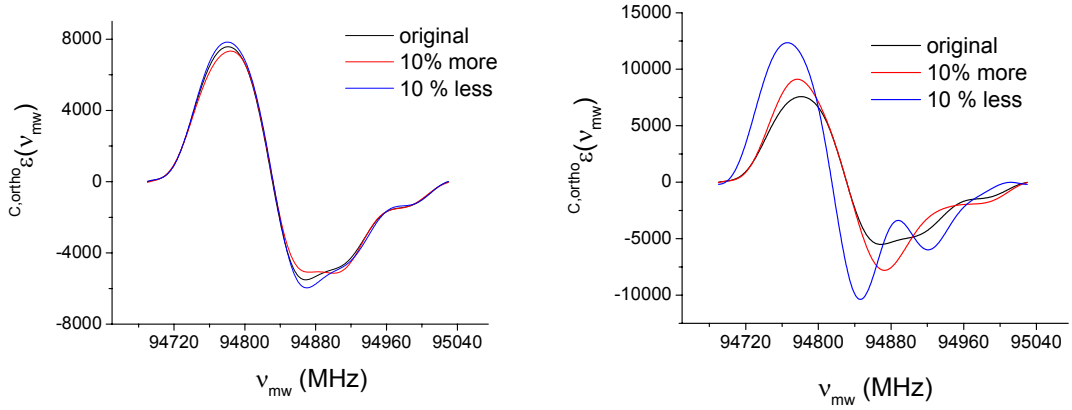

Figure S8: Effect of variations of the hyperfine and nuclear quadrupole principal components on the ^{13}C DNP sweep lineshape is demonstrated for *ortho* ^{35}Cl substituent of radical **1**: Hyperfine (left panel) and quadrupole (right panel). The effect of ±10% change in hyperfine coupling is found to be rather subtle. In contrast a 10% reduction in quadrupole coupling constant was found to introduce significant shift to low frequencies (right panel, blue line).